River Flow 2014 – Schleiss et al. (Eds)
© 2014 Taylor & Francis Group, London, ISBN 978-1-138-02674-2

transport over an hydraulically rough bed

Bruno O. Santos
Department of Civil Engineering and IMAR CMA, New University of Lisbon, Portugal

Mário J. Franca
Laboratoire de Constructions Hydrauliques, École Polytechnique Fédérale de Lausanne, Lausanne, Switzerland

Rui M.L. Ferreira
CEHIDRO, Instituto Superior Técnico—ULisboa, Portugal

ABSTRACT: Excess sediment production in the upper parts of catchments may result in important impacts over morphodynamics of gravel bed-rivers. By changing morphodynamics, sediment overfeeding may induce important changes in the structure of near-bed flow, mainly in what concerns exchange of momentum and mass between flow within the roughness elements and flow in the upper regions. It is not well-known how turbulent statistics, including those characterizing the bursting cycle, are affected by bed load transport, for mobile but geometrically similar beds. This study addresses this issue. It is aimed at evaluating the impacts of sediment transport on flow hydrodynamics, namely on statistics of turbulent coherent structures. In order to accomplish the proposed objective, laboratory tests were undertaken. Two-dimensional instantaneous flow velocity fields in the stream-wise and vertical directions were measured with Particle Image Velocimetry.

Two laboratory tests simulated a framework gravel bed with sand matrix and a framework gravel bed with sand matrix but with sediment transport imposed at near capacity conditions. The framework consists of coarse gravel whose diameters range between 0.5 cm and 7 cm and is kept immobile under the imposed flow conditions. The mobile sediments are sand with a mean diameter of 0.9 mm. For both tests, the quadrant threshold analysis technique was employed and shear stress distribution statistics were analyzed and discussed in what concerns their contribution and persistence.

In the case of mobile conditions, sweep events tend to govern the flow in the near-bed region. Relevant differences between mobile and sub-threshold beds are found in the wake of roughness elements, mostly for sweep statistics. In the presence of bed-load, ejection events decrease their participation in the shear stress production processes. This decrease in the ejection events contribution is partially balanced with an increase in the frequency of inward events.

1 INTRODUCTION

Bursting phenomena is a class of coherent structures occurring mainly in the near wall region. It is originated from a quasi-cyclic process composed of interactions in the four quadrants. These phenomena are responsible for the essential mechanism of generating turbulent energy and shear stress.

Pioneering works were performed by Kline et al. (1967), Kim et al. (1971), Grass (1971) and later by Nakagawa and Nezu (1977) where bursting phenomena was firstly identifyed. Major advances have been made in the characterization of organized turbulence with the appearence of innovative aquisition techniques, such as Laser Doppler Velocimetry (LDV) and Particle Image Velocimetry (PIV). The works of Gyr and Schmid (1997) concluded that the presence of intense intermittent sediment transport increases the extreme values of shear stress while the flow becomes more organized in the second and fourth quadrants, mainly increasing the importance of sweep events to turbulence production, while Ferreira et al. (2009) suggested that further research was needed to clarify the nature of feedback effects between turbulent flow organization and sediment fluxes.

Fundamental questions remain unsolved in what concerns flow organization under sediment transport conditions, specially in ejections and sweep events which are the major contribuitors to the Reynolds shear stress production among the bursting cycle.

The purpose of this work is to to contribute to the understanding of coherent structures that

govern the flow when in bed-load sediment transport conditions in the pythmenic region, over crests and in troughts. Organized turbulence investigated in both flows over hydraulically rough mobile and immobile porous boundaries.

A statistical characterization of events based on the Quadrant threshold method (Nakagawa and Nezu 1977) is performed in order to study each event preponderance in the sediment transport phenomena and to find a pattern in the event magnitude underthese same conditions.

Ejection and sweeps events are accounted in the flow organization and in order to characterize such events, parameters like event duration, maximum shear stress, transported momentum and period of occurence are considered through a statistical approach.

This paper is organizaed as follows: description of the laboratory facilities and instrumentation, description of the analysis methods, presentation of the experimental results and discussion, and conclusions.

2 CHARACTERIZATION OF THE PHYSICAL SYSTEM

The presence of coarse sediment entrained in the flow introduces some differences in the stream structure. Due to this, Ferreira et al. (2012) proposed a model, based on the one previously defended by Nikora et al. (2001), that features a longitudinal layer, the pythmenic region, where the flow is determined by the particular geometry of bed roughness elements and, possibly, the amount and size of moving particles. The main particularity in this model is that the regions overlap as the phenomena that characterize it do not cease to exist abruptly.

The outer layer is in the near-surface region where the flow is mainly governed by the influence of the surface, rather than the wall (Fig. 1).

In the inner region the flow is directly governed by the bed roughness in its lowermost region and indirectly in its uppermost region. Should the flow depth be sufficiently high, the overlapping between both outer and inner regions results in the logarithmic region, as the vertical profile of the longitudinal velocity is logarithmic.

The flow in the pythmenic layer is governed by the wall micro-topography. The overlapping region between pythmenic and inner layers results in a region at the highest crests elevation where the interaction between characteristics from both regions generates strong momentum fluxes in vertical direction.

The hyporeic region is below the pythmenic layer where the flow mainly depends on the void function.

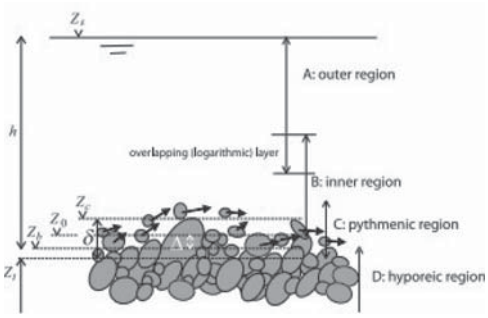

Figure 1. Flow structure proposed for permeable rough porous poorly sorted gravel-sand beds with sediment bed load. h stands for the flow depth, Z_b stands for the boundary zero elevation, Z_c stands for the highest crest elevation, Z_s stands for the elevation of the free-surface and Z_t is the elevation of the deepest through.

The overlapping between both hyporeic and pythmenic regions may not contribute to the mean flow, should the bed be deep.

3 LABORATORY FACILITIES AND INSTRUMENTATION

Experimental tests were performed recurring to the Recirculating Tilting Flume (CRIV), which is placed at the Laboratory of Hydraulics and Environment of Instituto Superior Técnico, Universidade de Lisboa.

The flume has a square cross section with 408 mm wide, 300 mm in height and its effective length is 12.5 m. It is composed of 10 glass panels with 0.5 m height, in each sidewall, that keep the fluids inside it and allow to acquire experimental data recurring to measurement means based on flow visualization.

The main structure is supported by columns and the upstream column is suitable of being raised or lowered in order to adjust the flume slope through means of a motorized system. Its slope adjustment ranges between –1/200 and +1/40.

The recirculation is made through a pressure circuit, incorporating a centrifugal pump with a maximum discharge of 220 m^3/h, measured by a electromagnetic low-meter.

Free surface oscilations are eliminated at the inlet by means of a wooden board. The water level and the uniform flow conditions in the subcritical regime are set and controlled by a venetian blind gate at the outlet which is tune using a screw pole.

At a distance of 2.5 m downstream from the inlet, a conveyor belt imposes a constant sediment feed. The belt is equipped with a structure that allows controlling the sediment discharge by regulating its velocity and the thickness and width

of the sediment streak. A polystirene board is used to eliminate any free surface disturbance resulting from the introduction of sediments in the stream.

These experimental tests demanded measurements of free surface elevation, bed topography and instantaneous flow velocity maps in both longitudinal and vertical directions. The free surface elevation and bed topography profiles were obtained recurring to a point gauge with 0.1 mm of precision while the instantaneous flow velocity maps were acquired non-intrusively through means of a Particle Image Velocimetry (PIV) system. The PIV system encompass a 30 mJ Nd: YAG SoLo 532 mm laser, a Charge Couple Device (CCD) camera with a resolution of 1600 × 1200 pixel and an aquisition system. The laser is shaped in a sheet through means of cylindrical lenses providing a thick sheet of light. The system operation is performed through a double cavity laser with time between pulses and sampling frequency controlled by the user.

4 EXPERIMENTAL TESTS

Two experimental tests were undertaken, which instantaneous flow velocity maps were collected, under uniform flow conditions. The tests were named S3 and S4, respectively in mobile bed and immobile bed conditions, and their main characteristics are shown in Table 1.

Table 1 presents flow characteristics for each test, S3 and S4, where Q stands for flow discharge, i is the bed slope and q_b is the volumetric sediment discharge. The bed is composed of gravel and sand with mean diameter and the geometric standard deviation respectively, $d_{50}^{g} = 28$, $\sigma_D^{g} = 1.4$ for gravel and $d_{50}^{s} = 0.9$, $\sigma_D^{s} = 1.6$ for sand.

In both tests the coarse-gravel elements were forming a 3D structure in the bed, whose interstices were filled with sand. This was achieved by water-working the bed during 30 hours to completely assure the armouring conditions. By filling the interstices, the thickness of the pythmenic layer is reduced and consequently the porosity in the substratum is reduced too.

In test S4 the filling sand is well stored below crests ensuring that sediment transport is completely inexistent under the imposed flow conditions, while in test S3 the sand presence in the bed was slightly increased, until the sand discharge achieves minimum transport capacity.

The bed is characterized by the parameters shown in Table 2, such as, elevation of the lowest trough, z_t, elevation of the highest crest, z_c, thickness of the pythmenic layer (Ferreira et al. 2012), $\delta = z_c - z_t$, bed porosity, λ_b and mean value of the void function, φ_m, which characterizes the rate of space that is occupied by the fluid in a planar area of the flow.

Uniform flow conditions were achieved by adjusting the downstream gates of the channel. Table 3 lists the mean flow characteristics.

The variable in Table 3 are Z_s the free surface elevation, while $h^{\star}$ is a reference flow depth for shear stress calculation purposes and is calculated as $h^{\star} = h - \delta(1-\varphi_m)$, U is the depth averaged mean flow velocity in the stream direction, calculated by $U = Q/B \cdot (Z_s - z_c)$, where B is the flume width.

The value of τ_0 stands for total shear stress and it is estimated from total shear stress profile. This profile is subjected to a liner regression in the linear segment and then extrapolated to the level of the mean void function, estimating total shear stress of the flow, τ_0, while $u_* = \sqrt{\tau_0/\rho^{(w)}}$.

The mean flow is also suscecpitle to be characterized by the non-dimensional parameters presented in Table 4. Froude number calculated by $Fr = U/\sqrt{g \cdot h}$, where U represents the depth-averaged mean flow velocity, g is the acceleration of gravity and h is the flow depth. The Reynolds number calculated by $Re = U \cdot h/\nu$, where ν is the viscosity of the water. The Shields parameter

Table 2. Geometrical characteristics of the bed.

Test	z_t (m)	z_c (m)	δ (m)	φ_m (–)	λ_b (–)
S3	0.107	0.146	0.039	0.7197	0.22
S4	0.090	0.144	0.053	0.6570	0.34

Table 3. Mean flow characteristics.

Test	Z_s (m)	h^* (m)	U (m/s)	τ_0 (Pa)	u^* (m/s)
S3	0.234	0.116	0.648	3.060	0.057
S4	0.246	0.137	0.557	3.924	0.062

Table 1. Main characteristics of experiments S3 and S4.

Test	Q (l/s)	i (–)	q_b (l/s)	h (m)
S3	23.3	0.0044	4.77×10^{-3}	0.127
S4	16.7	0.0044	2.08×10^{-3}	0.156

Table 4. Non-dimensional parameters.

Test	Fr	Re	ϑ^g	ϑ^s
S3	0.61	76606	0.008	0.223
S4	0.45	86843	0.009	0.269

is calculated for both gravel and sand sizes by $\vartheta^i = racu_*^2(\rho^{(i)}/\rho^w - 1)\cdot g\cdot d_{50}^i$, where u^* stands for friction velocity, ρ^w is the water density, ρ^i is sand or gravel density, and d_{50}^i is the mean diameter of sand or gravel.

5 DATA ANALYSIS

5.1 *Conditional sampling and detection criteria*

The conditional sampling organizes the shear stresses and helps in the identification of events occuring in the bursting cycle. The quadrant threshold method was choosen to establish the detection criteria because it provides good results in the identification of events simply based on the fluctuation of instananeous flow velocities in both u' and v' directions, respectively longitudinal and vertical. The fluctuation of instantaneous flow velocity results from subtracting the time averaged flow velocity from the instantaneous flow velocity fields. This method was initially described by Nakagawa and Nezu (1977) but recently, Ferreira et al. (2009) proposed some changes that were considered in this work.

The Quadrant threshold technique involves thresholding valuable data accordingly to each quadrant. The thresholds are controlled by the constants σ_h, σ^+ and σ^- which are calculated using Equations 1 and 2.

$$\sigma_h = H \times u_{rms} \times w_{rms} \tag{1}$$

$$\sigma^{\pm} = \pm 2.5 \times u_{rms} \tag{2}$$

where H represents the hole size and, u_{rms} and w_{rms} are the root mean square of the instantaneous flow velocity, respectively in longitudinal and vertical directions.

In this method of detection the values of fluctuation of the instantaneous flow velocity are considered and events of Outward, Ejection, Inward and Sweep are identified based on the following domains of occurrence:

i. Outward interactions: $Q_{out} = \{u', w' \in \mathbb{R} : u' > 0 \wedge w' > \frac{\sigma_h}{u'} \wedge u' < \sigma^+\}$;
ii. Ejection interactions: $Q_{ej} = \{u', w' \in \mathbb{R} : u' < 0 \wedge \{w' > \frac{\sigma_h}{|u'|} \vee u' < \sigma^-\}\}$;
iii. Inward interactions: $Q_{in} = \{u', w' \in \mathbb{R} : u' < 0 \wedge w' < 0 \wedge |w'| > \frac{\sigma_h}{|u'|} \wedge u' > \sigma^-\}$;
iv. Sweep interactions: $Q_{sw} = \{u', w' \in \mathbb{R} : u' > 0 \wedge \{\{w' < 0 \wedge |w'| > \frac{\sigma_h}{u'}\} \vee u' > \sigma^+\}\}$.

An example of the quadrant threshold techinique is shown in Figure 2.

Due to the problem of treating consecutive events of smaller scale as independent events results in an incorrect approach. To avoid that in the boundary

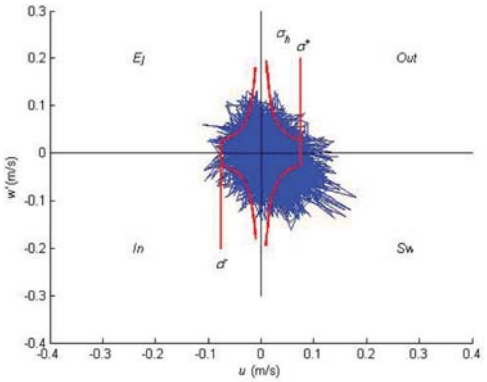

Figure 2. Example of the Quadrant threshold techinique applied to a randomly choosen set of data.

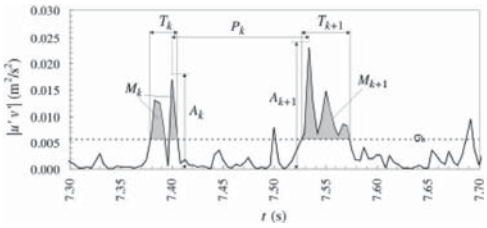

Figure 3. Detailed shear stress time series with parameters that characterize events.

regions, a consecutive set of smaller scale events is elegible as a single major event if the persistence of u' is well correlated with the persistence of the event, as shown by Ferreira et al. (2009).

5.2 *Event statistics*

Parameters are achieved by calculating geometrical characteristics of the event, over a time series, as presented in Figure 3. The maximum shear stress (A) is the elevation of the highest peak, transported momentum (M) is the area delimited by the time series and the threshold, duration (T) is the lenght of the event and period (P_c) is the time between consecutive events, measured between centroids.

A statistical approach is then applied over these parameters for each sort of event and achieving valuable data on how a certain event is reproduced in time at a certain location in the flow.

6 RESULTS AND DISCUSSION

A statistical distribution of the parameters that characterize sweep and ejection events are assessed in both immobile and mobile bed conditions.

The analysis was made at several positions of the flow velocity maps as represented in Figure 4.

The points considered for results were chosen accordingly to the physical system proposed by Ferreira et al. (2012) which is indicated for porous mobile beds in steady free-surface flows with transported sediments as bed load.

The points marked as (1,2) and (1,4) were adopted because they are far enough from the bed, standing clearly in the outer region where the flow structure does not depend on the wall. Points (2,2) and (2,4) coincide correspond to the interception between the outer layer and the inner regions. Points (3,1), (3,2), (3,3) and (3,4) are standing at the highest crest level at the interface between inner and pythmenic layers. They can evaluate the influence over the flow caused by the crest itself and bythe mobile bed. Other points were chosen into the troughs; Because they are undoubtedly in the pythmenic layer they establish a comparison between the effect of the trough itself and the effect of a mobile bed. Point (4,4) was considered because it is well above the lowest troughs. The effects of the hyporheic and pythmenic regions can be noticed in points (5,1), (5,3) and (5,4) because they were chosen at the closest available points to the bed, where data is acquirable by PIV means.

In the remainder of this work, three points are presented in detail, namely are (3,2), (3,3) and (5,4). These points constitute a sample of the remaining points, as they stand in the most important regions of the flow for this work purposes.

As the value of the hole size is important to establish a threshold in the quadrant analysis method, a criteria was applied to choose it. The hole size value was the one for which the transported momentum produced by outward and inward interactions is not greater than 10% of its total value at that particular point. The adopted hole size corresponds to a value of $H = 0.4$ and this hole size was used to compute the statistics of ejection and sweep events shown in the remaining results.

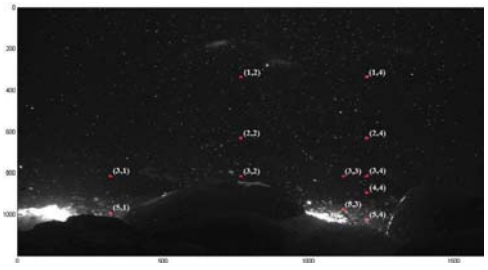

Figure 4. Location of the reference points which were considered.

As a first approach, the average and extreme values of the considered parameters, namely, event duration, maximum shear stress, transported momentum and period, were considered and analysed. Then, a probability density function was employed to complete the characterization of the flow.

The ejection and sweep events were computed for mobile and immobile bed, obtaining the statistical distribution of flow parameters that characterize them and allowing to compare experiments between both bed conditions.

6.1 *Point (3,2)—Over the crest, in the interception between outer and inner regions*

Figure 5 shows that small values of maximum shear stress (A), and transported momentum (M) exhibit larger frequencies in mobile bed conditions. This indicates that sediment transport may contribute to break the coherence of events and thus increase the frequency of small events.

At this reference position, Table 5 shows that the duration of events do not present major differences between immobile and mobile conditions, but the period of sweep events slightly decreases while the opposite occurs with ejection events in mobile conditions.

6.2 *Point (3,3)—At the crest level but over the trough*

Point (3,3) stands in the region governed by characteristics of the inner and pythmenic layers. At this point, the average values of A and M increase in comparison with Table 5, however, the average

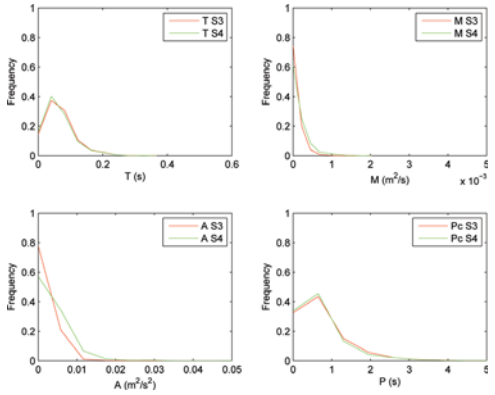

Figure 5. Histograms of duration (T), maximum shear stress (A), transported momentum (M) and period (P_c), of ejection events at reference point (3,2). Comparison of data sets S4, immobile bed in green and S3, mobile bed in red.

Table 5. Average and extreme values of the parameters calculated at reference point (3,2) in both mobile (S3) and immobile (S4) bed conditions. Where T represents the duration, A is the maximum shear stress, M is transported momentum and P_c is the period of events.

	Reference point (3,2)			
	T (s)	A (m^2/s^2)	M (m^2/s)	P_c (s)
Ejections				
Avr S3	0.07	0.0019	0.0001	0.70
S4	0.06	0.0036	0.0002	0.67
Max S3	0.37	0.0157	0.0013	4.68
S4	0.31	0.0525	0.0020	5.87
Sweeps				
Avr S3	0.07	0.0018	0.0001	0.65
S4	0.07	0.0041	0.0002	0.70
Max S3	0.39	0.0195	0.0019	4.16
S4	0.41	0.0455	0.0037	5.17

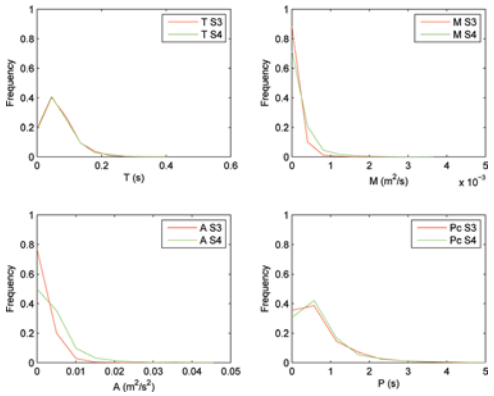

Figure 6. Histograms of duration (T), maximum shear stress (A), transported momentum (M) and period (P_c), of sweep events at reference point (3,2). Comparison of data sets S4, immobile bed in green and S3, mobile bed in red.

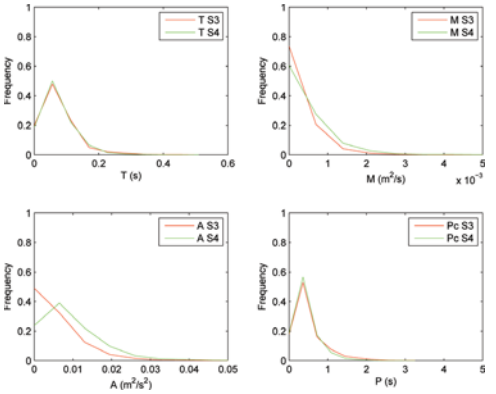

Figure 7. Histograms of duration (T), maximum shear stress (A), transported momentum (M) and period (P_c), of ejection events at reference point (3,3). Comparison of data sets S4, immobile bed in green and S3, mobile bed in red.

Table 6. Average and extreme values of the parameters calculated at reference point (3,3) in both mobile (S3) and immobile (S4) bed conditions. Where T represents the duration, A is the maximum shear stress, M is transported momentum and P_c is the period of events.

	Reference point (3,3)			
	T (s)	A (m^2/s^2)	M (m^2/s)	P_c (s)
Ejections				
Avr S3	0.07	0.0056	0.0003	0.48
S4	0.07	0.0091	0.0005	0.42
Max S3	0.47	0.0481	0.0035	3.26
S4	0.51	0.0586	0.0063	2.93
Sweeps				
Avr S3	0.08	0.0045	0.0003	0.47
S4	0.07	0.0107	0.0005	0.45
Max S3	0.49	0.0357	0.0036	4.00
S4	0.35	0.0762	0.0076	4.40

values of period P_c decrease. The presence of bed load exhibit a decrease in values of A and M, for both ejection and sweep events while P_c remains invariable.

Regarding the extreme values of the four parameters analysed, the maximum shear stress and transported momentum values keep the behaviour from the average values. The maximum values of period decrease for sweep events and present an increase forejection events.

Figure 7 corroborates Table 6, as ejection durations and period are not perturbed at all by mobile bed. The frequency of small A and M values in mobile bed conditions is also supported by Table 6.

Figure 8 shows a similar behaviour between sweep and ejection events at this point.

6.3 *Point (5,4)—In the overlapping between pythmenic and hyporheic regions*

Point (5,4) is placed in the deepest trough, where pythmenic region overlaps the hyporheic region. At this point ejection events present a marked decrease in mobile bed conditions as shown by A and M values in Table 7. Sweep events also decrease in these values but not as much as ejections, indicating that at this point the shear stress is mainly produced by sweep events. The values of duration (T)

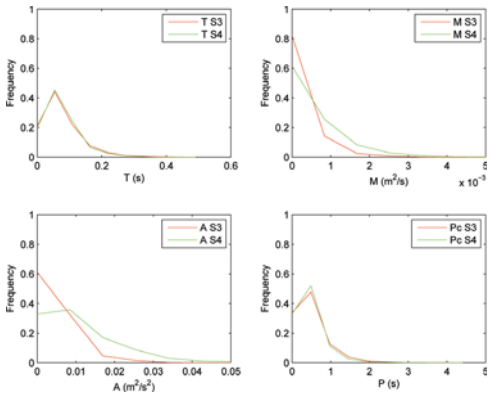

Figure 8. Histograms of duration (T), maximum shear stress (A), transported momentum (M) and period (P_c), of sweep events at reference point (3,3). Comparison of data sets S4, immobile bed in green and S3, mobile bed in red.

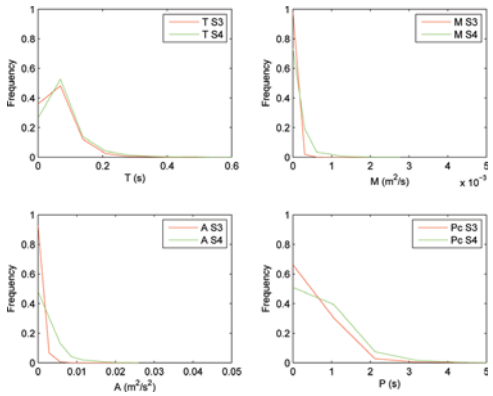

Figure 9. Histograms of duration (T), maximum shear stress (A), transported momentum (M) and period (P_c), of ejection events at reference point (5,4). Comparison of data sets S4, immobile bed in green and S3, mobile bed in red.

Table 7. Average and extreme values of the parameters calculated at reference point (5,4) in both mobile (S3) and immobile (S4) bed conditions. Where T represents the duration, A is the maximum shear stress, M is transported momentum and P_c is the period of events.

	Reference point (5,4)			
	T (s)	A (m^2/s^2)	M (m^2/s)	P_c (s)
Ejections				
Avr S3	0.06	0.0005	0.00002	0.52
S4	0.08	0.0027	0.00014	0.71
Max S3	0.52	0.0067	0.00050	9.54
S4	0.63	0.0260	0.00277	4.50
Sweeps				
Avr S3	0.0727	0.0019	0.0001	0.59
S4	0.0798	0.0038	0.0002	0.73
Max S3	0.46	0.0209	0.0018	6.47
S4	0.48	0.0546	0.0042	5.34

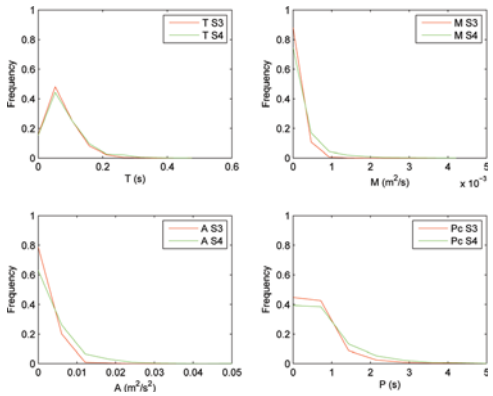

Figure 10. Histograms of duration (T), maximum shear stress (A), transported momentum (M) and period (P_c), of sweep events at reference point (5,4). Comparison of data sets S4, immobile bed in green and S3, mobile bed in red.

and P_c also show a decrease which is not important if compared to the remaining parameters.

Table 7 shows that extreme values present the same tendency as average values.

Figure 9 shows a decrease in the contribution of ejection events to the shear stress production process with a marked increase in small A and M values frequency in bed load conditions. Values of T and P_c also decrease which results in a smaller contribution of this event to the production of shear stress.

Analysing Figure 10 which stands for sweep events, there is a similar behaviour as the one described for ejections. However, Table 7 proves that despite the decrease in T and M, sweep events continue to be more important than ejection events in the shear stress production process. The average values of M at this reference position, shows that in the near wall region the flow is mainly governed by sweep events as stated by Gyr and Schmid (1997).

The experiment with mobile sediments shows that the sweep and ejection events are both affected, however, ejections are much more affected than sweep events in the pythmenic region.

7 CONCLUSIONS

The analysis of the laboratorial data were considered to evaluate the effect of sediment transport in

the near bed region over the coherent structures that characterize the flow in conditions of open channel flow with porous rough bed and poorly sorted gravel-sand mixture.

The data was processed by applying the quadrant analysis method, leading to an approach through the statistics of the duration, maximum shear stress, transported momentum and period of each event.

The discussion of these results lead to the conclusion that:

1. In the overlapping layer, between inner and pythmenic regions, which stands over the crest, the flow tends to be isotropic in mobile bed conditions. The events are equally distributed between the four quadrants and share responsibilities in the processes of shear stress production;
2. In the pythmenic region, standing into the through, mobile bed conditions lead to a situation where ejection and sweep events are responsible for the shear stress production processes with sweep events assuming a main role;
3. Generally, the sediment transport of sand decreases the transported momentum and maximum shear stress values but increases their frequency of occurrence in time;
4. The analysis of the probability distribution function (pdf) of both ejections and sweeps, especially in the pythmenic region, it is apparent that the effect of sediment transport is the reduction of the frequency of large events and the increase of the frequency of small events. This may be due to breaking of eddy coherence by sediment motion;
5. It is also concluded that the ejection events suffer the more important decreases due to sediment transport in the near bed region. This happens generally in the pythmenic region.

ACKNOWLEDGEMENTS

This work was partially funded by FEDER, program COMPETE, and by national funds through Portuguese Foundation for Science and Technology (FCT) project RECI/ECM-HID/0371/2012.

REFERENCES

Ferreira, R.M.L., M.J. Franca, J.G.A. B. Leal, & A.H. Car-doso (2012). Flow over rough mobile beds: Friction factor and vertical distribution of the longitudinal mean velocity. *Water Resources Research 48*(W011126).

Ferreira, R.M.L., M.J. Franca, J.G.B. Leal, & A.H. Cardoso (2009). Organized turbulence over mobile and immobile hydraulically rough boundaries. In *35rd IAHR Congress*, Van-couver, British Columbia, Canada, pp. 36–43. IAHR.

Grass, A.J. (1971). Structural features of turbulent flow over smooth and rough boundaries. *Journal of Fluid Mechanics 50*(02), 233–255.

Gyr, A. & A. Schmid (1997). Turbulent flows over smooth erodible sand beds in flumes. *Journal of Hydraulic Research 35*(4), 525–544.

Kim, H.T., S.J. Kline, & W.C. Reynolds (1971). The production of turbulence near a smooth wall in a turbulent boundary layer. *Journal of Fluid Mechanics 50*(01), 133–160.

Kline, S.J., W.C. Reynolds, F.A. Schraub, & P.W. Runstadler (1967). The structure of turbulent boundary layers. *Journal of Fluid Mechanics 30*(04), 741–773.

Nakagawa, H. & I. Nezu (1977). Prediction of the contributions to the reynolds stress from bursting events in open-channel flows. *Journal of Fluid Mechanics 80*(01), 99–128.

Nikora, V., D. Goring, I. McEwan, & G. Griffiths (2001). Spatially averaged open-channel flow over rough bed. *Journal of Hydraulic Engineering 127*(2), 123–133.